

The effects of airmass history on new particle formation in the free troposphere: case studies

D. R. Benson¹, Li-Hao Young¹, Shan-Hu Lee¹, T. L. Campos², D. C. Rogers², and J. Jensen²

¹Kent State University, Department of Chemistry, Kent, OH, USA

²National Center for Atmospheric Research, Earth Observing Laboratory, Broomfield, CO, USA

Received: 4 September 2007 – Published in Atmos. Chem. Phys. Discuss.: 8 October 2007

Revised: 12 March 2008 – Accepted: 20 May 2008 – Published: 18 June 2008

Abstract. Recent aircraft studies showed that new particle formation (NPF) is very active in the free troposphere. And, these observations lead to a new question: when does NPF *not* occur? Here, we provide case studies to show how different meteorological parameters affect NPF in the upper troposphere, using the aerosol size distributions measured at latitudes from 18° N–52° N and altitudes up to 14 km during the NSF/NCAR GV Progressive Science Missions. About 95% of the total samples showed the NPF feature with median number concentrations of particles with diameters from 4 to 9 nm (N_{4-9}), $288 \pm 199 \text{ cm}^{-3}$, and the total particle number concentrations with diameters from 4 to 2000 nm (N_{4-2000}), $500 \pm 259 \text{ cm}^{-3}$. Surface areas were in general very low in the free troposphere, $1.58 \pm 0.87 \mu\text{m}^2 \text{ cm}^{-3}$, which in part explains the high frequency of NPF measured in this region, but there was no distinctive difference in surface area for the NPF and non-NPF cases. Our case studies show that rather airmass history is more important for nucleation in this region. Weak- or non-events did not display uplifting of airmasses. On the other hand, strong NPF events were usually associated with uplifting of airmasses, although there were also NPF cases in which uplift did not occur, consistent with the previous observations (Young et al., 2007). NPF tends to easily occur in the free troposphere because of low surface areas and low temperatures (Carslaw and Kärcher, 2006), but because of the low aerosol precursors in this region, vertical motion (that can bring higher concentrations of aerosol precursors from low altitude source regions to higher altitudes) can play a critical role. Latitude dependence of new particles also shows higher particle concentrations in the midlatitude and subtropics tropopause region than in the tropics, consistent with Hermann et al. (2003).

1 Introduction

Recent aircraft studies showed new particle formation (NPF) in the free troposphere and lower stratosphere (de Reus et al., 1998, 1999; Nyeki et al., 1999; Twohy et al., 2002; Lee et al., 2003; Young et al., 2007) with high frequencies (up to 86–100%) (Young et al., 2007) and strong magnitudes (up to $45\,000 \text{ cm}^{-3}$) (Twohy et al., 2002). Hermann et al. (2003) have provided so far the most comprehensive statistical analysis of NPF in the Northern Hemisphere tropopause region from three-year aircraft measurements; elevated particle number concentrations of $1500\text{--}8000 \text{ cm}^{-3}$ were frequently observed in a wide range of latitudes (5° N–50° N). Twohy et al. (2002) showed especially high number concentrations of new particles up to $45\,000 \text{ cm}^{-3}$ in the midlatitudes, associated with deep convection. Minikin et al. (2003)'s aircraft studies showed relatively high concentrations of Aitken mode particles (up to 1000 cm^{-3}) even in the Southern Hemisphere, where the anthropogenic emission of SO₂ is much lower than in the Northern Hemisphere; their comparison of particle number concentrations in the Northern and Southern Hemisphere indicates that new particles are directly related to aerosol precursor sources. NPF events take place near or in orographic clouds (Wiedensohler et al., 1997; Mertes et al., 2005) and stratus clouds (Hegg et al., 1992) during the nighttime, and even in cirrus clouds (Lee et al., 2004). As NPF was observed in a wide range of the free troposphere and lower stratosphere (Ström et al., 1999; Twohy et al., 2002; Hermann et al., 2003; Minikin et al., 2003; Lee et al., 2003, 2004; Young et al., 2007), it is also important to understand when NPF *does not* occur or when weak NPF occurs.

We present results from NPF studies during the National Science Foundation (NSF) and National Center for Atmospheric Research (NCAR) NSF/NCAR GV Progressive Science Missions. The GV is also known as HIAPER, the High-performance Instrumented Airborne Platform for



Correspondence to: Shan-Hu Lee
(slee19@kent.edu)

Table 1. The median values of the measured particle concentration from 4–9 nm (N_{4-9}), the particle concentration from 4–2000 nm (N_{4-2000}), and other key meteorological parameters during the entire NSF/NCAR GV Progressive Science Missions. All 7 research flights are included here. The median absolute deviation values are also included. NPF indicates NPF. In total, 5181 data points of 30 s average data are included here.

	All Days	NPF	Non-NPF
N_{4-9} (cm^{-3})	275±198	288±199	4.93±4.88
N_{4-2000} (cm^{-3})	457±273	500±259	60.8±42.3
Surface Area ($\mu\text{m}^2 \text{cm}^{-3}$)	1.58±0.87	1.52±0.84	2.32±1.49
Temperature (K)	228±11	227±8	244±29
Relative Humidity Over Ice (%)	13.3±11.0	11.4±8.8	24.9±24.0
Potential Temperature (K)	325±14	327±12	310±26
H ₂ O Mixing Ratio (ppmv)	115±75	102±58	423±398
Altitude (km)	9.52±2.31	9.87±1.94	5.67±4.72
Fraction of samples (%)	100	95	5

Environmental Research. The Progressive Science Mission was the first science mission onboard the GV and there were seven days of research flights (Young et al., 2007). There is the Part I paper by Young et al. (2007) that used two days of measurements in the midlatitude tropopause region (on 1 and 7 December 2005) from this mission to show how stratosphere and troposphere air mixing enhances NPF. The present study is the Part II paper, and we want to investigate when no-/weak- NPF takes place. There is also a third manuscript (Lee et al., 2008) that discusses nighttime ultra-fine particles observed from GV.

2 NSF/NCAR GV Progressive Science Missions

The NSF/NCAR GV Progressive Science Mission NPF studies took place from 21 November to 19 December 2005 in Broomfield, Colorado. The flights covered the western half of the United States, and parts of Canada and Mexico in latitude from 18° N to 62° N and in longitude from 92° W to 130° W. There were three days of nighttime NPF experiments (2, 12 and 19 December 2005) in order to investigate the effects of sun exposure (Lee et al., 2008). Nighttime studies in this region are rare.

Aerosol sizes and concentrations were measured with the University of Denver nuclei mode aerosol size spectrometer (NMASS) and focused cavity aerosol spectrometer (FCAS). These instruments are described in detail elsewhere (Jonsson et al., 1995; Brock et al., 2000; Lee et al., 2003, 2004; Young et al., 2007) and have been used for NPF studies in the upper troposphere and lower stratosphere previously (Lee et al., 2003, 2004; Young et al., 2007). Briefly, NMASS has five condensation nucleus counters that measure cumulative number concentrations of aerosols larger than 4, 8, 15, 30 and 60 nm, respectively. FCAS is a light scattering instrument and sizes aerosols from 90 to 2000 nm. Using an inversion

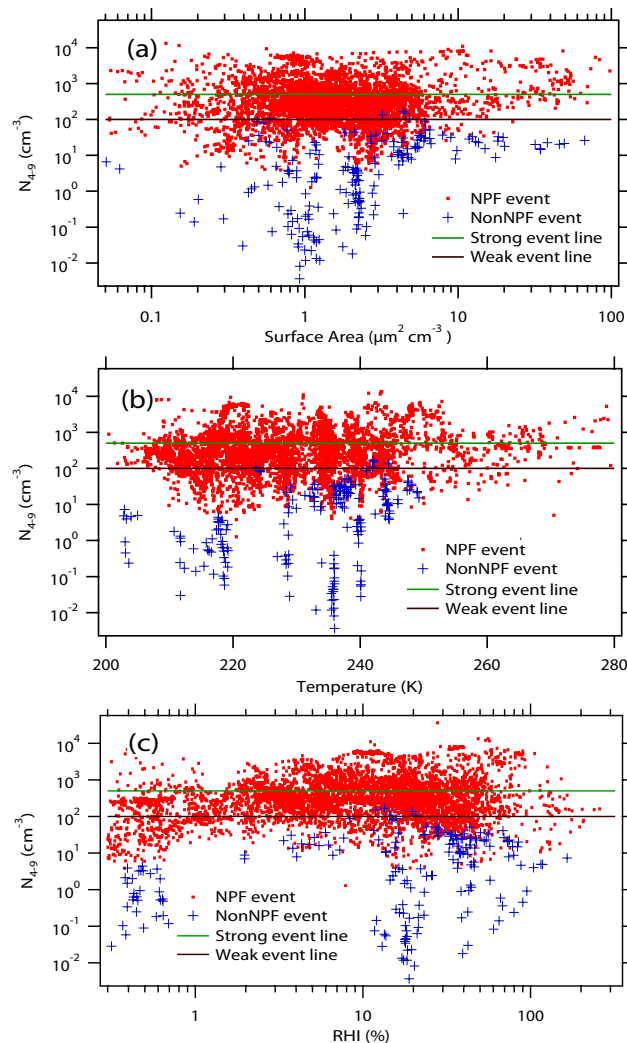


Fig. 1. The measured N_{4-9} as a function of surface area, temperature and RHI during the entire NSF/NCAR GV Progressive Science Mission. All 7 research flights are included here. The data are split into two categories, NPF (red circles) and non-NPF (blue crosses), as discussed in the text. The horizontal bars indicate the level of the strong- ($N_{4-9} > 500 \text{ cm}^{-3}$) (green) and weak-NPF ($N_{4-9} < 75 \text{ cm}^{-3}$) (brown); note that the weak event line also is nearly the same as that the upper limit of the non-NPF N_{4-9} , indicating that both non- and weak-events have sufficiently low N_{4-9} .

algorithm, size distributions from 4 to 2000 nm are obtained. The inversion also includes sampling efficiency, anisokinetic inlet effects, and diffusion loss etc.

The criteria for NPF are (i) $N_{4-9} > 1 \text{ cm}^{-3}$, (ii) more than 1/15 of N_{4-2000} are N_{4-9} , and (iii) particles from 4 to 6 nm (N_{4-6}) are higher than those from 6 to 9 nm (N_{6-9}) (Young et al., 2007). A non-NPF event is defined when at least one of these three criteria is not satisfied. Non-events tended to have size distributions without a peak in the size range $< 10 \text{ nm}$, a

clear indication of more aged aerosols than for NPF cases (Fig. 3c). Each NPF event is further classified as a strong or weak event by comparing with “background” concentrations, which are referred to as the median concentration values from all events shown in Table 1. Strong events are for the cases when $N_{4-9} > 500 \text{ cm}^{-3}$ (which is approximately the same value as that one median absolute deviation value higher than the median N_{4-9} for all events, $(275+198) \text{ cm}^{-3}$ in this case; similarly to Young et al. (2007)); weak events are defined when $N_{4-9} < 100 \text{ cm}^{-3}$ (one median absolute deviation value lower than the median N_{4-9} for all events, which is $(275-198) \text{ cm}^{-3}$, and we took 100 cm^{-3} here for simplicity). As shown in Fig. 1, weak- and non-NPF cases show a similar upper level of N_{4-9} , indicating that even though these two cases may have different size distributions (e.g., N_{4-6} vs. N_{6-9}), they both have low N_{4-9} . Previous NPF studies in the free troposphere made by other investigators have used the criterion that the measured total CN concentrations are higher than the background CN concentrations to identify NPF cases (Twohy et al., 2003 and numerous references cited therein), for example. In comparison, our criteria for NPF are more quantitative, yet consistent with these cited studies. For example, our non-NPF samples had much lower N_{4-9} and N_{4-2000} than the median concentrations from all days of experiments (Table 1) (that is, background concentrations) so they will also be non-NPF cases even with the NPF criterion used in these cited studies.

There were only less than 2% of the measurement data from this mission showed RH values greater than 100%. All case studies presented here were taken from cloud free sections of the flight (e.g., $\text{RH} < 60\%$) so new particles were not affected by clouds. Our previous studies also have shown that shattering of clouds in the inlet of the NMASS and FCAS instruments has little effects on the measured aerosol number concentrations (while there are some effects on mass concentrations) (Lee et al., 2004), so the measured new particles were unlikely affected by cloud processing.

3 Results

3.1 Overall

Table 1 summarizes the measured particle concentrations and meteorological conditions during this mission, including the measured N_{4-9} , N_{4-2000} , surface area density of preexisting aerosols, temperature, relative humidity over ice (RHI), the potential temperature, water mixing ratio, and altitude, along with the fraction of samples that satisfy (thus NPF), or do not satisfy (non-NPF), the NPF criteria. Overall, there were 95% of NPF and 5% of non-NPF cases during the entire Progressive Science Missions (Table 1). Furthermore, 30% of NPF cases were strong-NPF and 25% were weak-NPF. For NPF events, the median N_{4-9} value was $288 \pm 199 \text{ cm}^{-3}$ and the median N_{4-2000} was

$500 \pm 259 \text{ cm}^{-3}$. On the other hand, non-NPF events had a median N_{4-9} of $4.93 \pm 4.88 \text{ cm}^{-3}$ and a median N_{4-2000} of $60.8 \pm 42.3 \text{ cm}^{-3}$, both much lower than the overall N_{4-9} of $275 \pm 198 \text{ cm}^{-3}$ and N_{4-2000} of $457 \pm 273 \text{ cm}^{-3}$. The important feature here is that a small fraction of measurements (5%), the non-NPF cases, showed an obvious and large deviation from the N_{4-9} median. Surface area concentrations were very low in this region, $1.58 \pm 0.87 \mu\text{m}^2 \text{ cm}^{-3}$. For NPF events surface areas were $1.52 \pm 0.84 \mu\text{m}^2 \text{ cm}^{-3}$, and for non-events $2.32 \pm 1.49 \mu\text{m}^2 \text{ cm}^{-3}$; however, the ranges of surface area were in fact the same for NPF and non-NPF events (Fig. 1). Our low surface areas are consistent with other studies ($4-6 \mu\text{m}^2 \text{ cm}^{-3}$ on average (Young et al., 2007), $3.4 \pm 1.7 \mu\text{m}^2 \text{ cm}^{-3}$ (Lee et al., 2003) and less than $10 \mu\text{m}^2 \text{ cm}^{-3}$ (Twohy et al., 2003; Carslaw and Kärcher, 2006)) and these low surface areas in general also explain the high frequency of NPF observed in this region. The higher median surface area for non-NPF is probably related to the fact that most of the non-NPF events were measured in the lower altitudes (Fig. 1b and c and Table 1). For example, for the non-event samples, the median temperature was $\sim 244 \text{ K}$, higher than that for NPF cases ($\sim 228 \text{ K}$) (Table 1).

Our case studies discussed below will show weak- or non-NPF events did not show uplifting of the air mass, whereas strong NPF cases were closely associated with uplifting. In the present study, uplifting of the air mass is defined based on the NOAA HYSPLIT backward trajectory outputs (e.g., air mass altitude dependence with time) (Draxler and Rolph, 2003). Uplifting is referred to as the cases when the air mass was uplifted from a lower altitude, usually less than 2 km above ground level, to higher altitudes at an uplift rate greater than 3 km per day and the air mass was exposed to these low altitude source regions for at least 2 days before the vertical motion. On the other hand, if this rate was less than 3 km per day or if the air mass spent less than two days at an altitude of 2 km or less, we considered such a case as a non-uplifting event. It is noted that this “uplifting” process is slightly different from the conventional “convection”, which is usually defined as a small scale process on the order of kilometers or less in size (the model output from NOAA HYSPLIT calculations only has a grid resolution of 1 degree and cannot truly resolve convective systems).

HYSPLIT trajectories were run for a large number of cases other than those presented in two case studies in Sects. 3.2 and 3.3. However, because of the tremendous amount of data points we did not calculate for each individual data point. Also, when calculating HYSPLIT trajectories, one can only input the UTC time in hours for the starting time and our measurements were in 1 s and the data presented here were averaged in 30 s. Regardless, for NPF events (Table 1), in general it seemed that the majority of the time (>50%) the events displayed some degree of uplift. On the other hand, all non-NPF events found in the free troposphere region did not experience uplifting of air masses (Sect. 3.2).

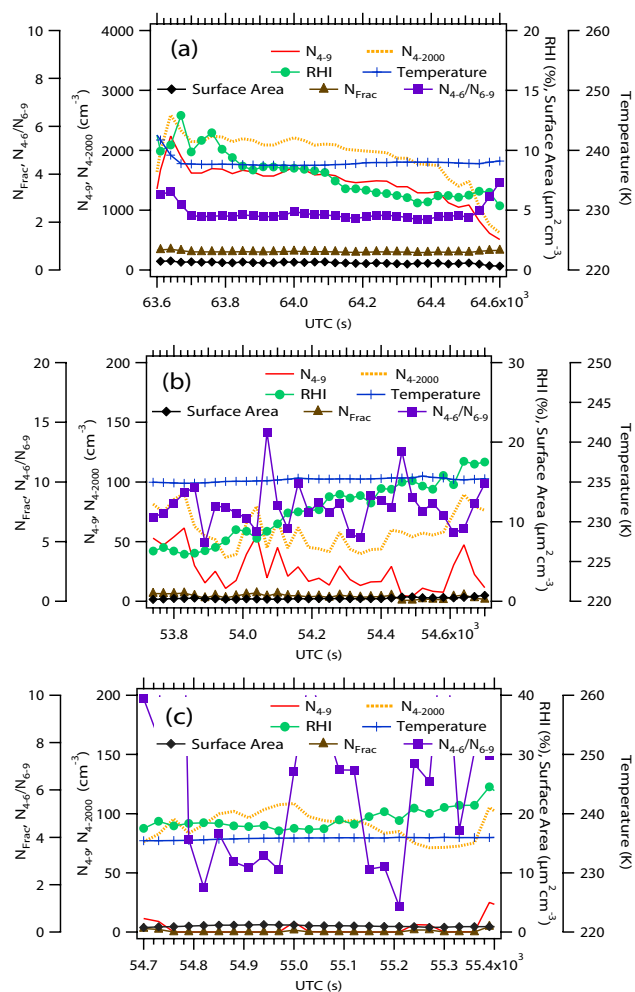


Fig. 2. The measured total particle number concentration (N_{4-2000}), ultrafine particle concentration (N_{4-9}), fraction of N_{4-9} in N_{4-2000} (N_{Frac}), ratio of the particle number concentration in the size range from 4 to 6 nm (N_{4-6}) over that from 6 to 9 nm (N_{6-9}), surface area, temperature and relative humidity over ice (RHI) as a function of universal time for several different events that were observed on 19 December 2005. (a) A strong NPF event observed during the day which occurred at 57° N, 116° W, 7.6 km and temperatures around 238 K. (b) A weak NPF event observed during the day which occurred at 50° N, 112° W, 8.0 km and temperatures around 235 K. (c) A non NPF event observed during the day which occurred at 52° N, 113° W, 8.0 km and temperatures around 237 K. See Fig. 2 for measured aerosol size distributions and Fig. 3 for backward trajectory calculations.

3.2 Case Study I (19 December 2005): Strong-, Weak-, and Non-NPF Events

To understand how different meteorological parameters affect NPF, a variety of types of NPF events must be analyzed including strong-, weak- and non-events. However, because there were only 186 data points (5%) that showed

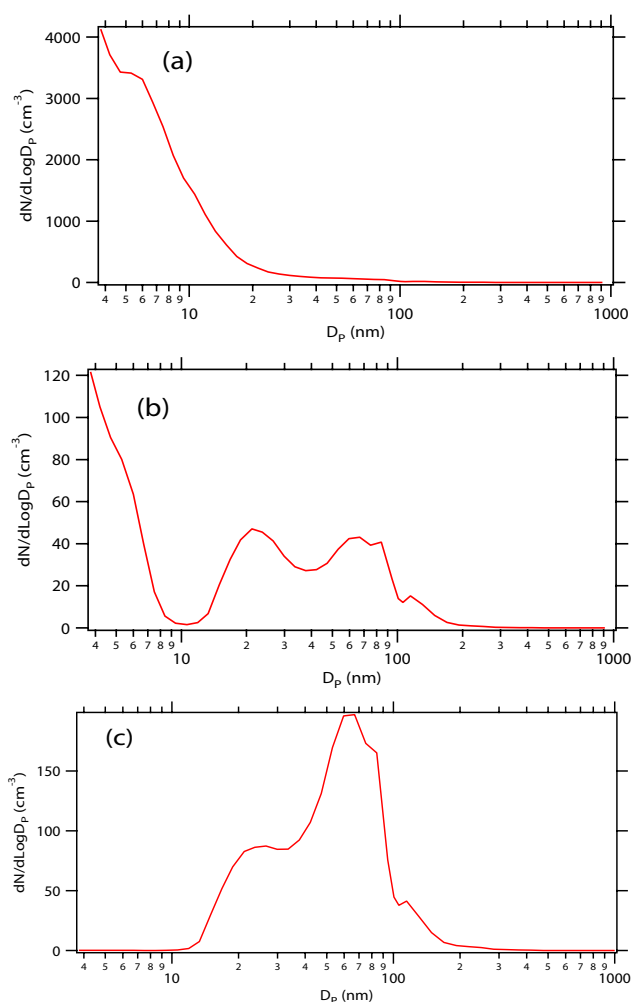


Fig. 3. The measured, average particle size distributions for the events shown in Fig. 2. The letters here correspond to those from Fig. 2 and each distribution is for the time period shown for the corresponding event from Fig. 2. The dip at ~ 100 nm in the size distribution comes from the inversion program when combining the NMAS and the FCAS data together and may not be representative of the actual aerosols sizes. The same is true for Fig. 6. The size mode at 20 nm or 70 nm (b and c) is representative of more aged particles that grew from newly formed fresh particles.

absolute non-NPF events (Table 2) and some of these data points were also rather sporadically distributed, we provide here only one case study including a non-NPF event. Figure 2 shows strong- (a) weak- (b), and non-NPF (c) event cases, for the measured N_{4-2000} , N_{4-9} , fraction of N_{4-9} in N_{4-2000} (N_{Frac}), ratio of the particle number concentration in the size range from 4 to 6 nm (N_{4-6}) over that from 6 to 9 nm (N_{6-9}) (N_{4-6}/N_{6-9}), surface area, temperature and RHI as a function of universal time for 19 December 2005's flight. On this day, the GV flew north to latitude 62° N before sunrise and returned to Colorado after sunrise, returning

Table 2. The meteorological parameters derived from the five day NOAA HYSPLIT trajectory calculations for the case studies used in the present study. Median, maximum, and minimum values of the altitude, temperature, RHI, cumulative precipitation and cumulative solar flux intensity are shown.

Case Study I: 19 December 2005											
Event	Altitude (km)			Temperature (K)			RHI (%)			Prec. (mm)	Solar Flux (kW m^{-2})
	Med.	Min	Max	Med.	Min	Max	Med.	Min	Max	Cumul.	Cumul.
Non	7.5	6.9	9.0	242	220	248	57	29	90	1.8	17.2
Weak	6.4	2.2	9.2	251	219	284	74	12	99	10.2	19.3
Strong	2.2	0.8	9.0	276	216	288	72	27	92	12.4	22.6
Case Study II: 12 December 2005											
Weak	8.3	6.2	9.9	244	223	265	40	2	95	8	58.5
Strong	0.6	0.1	10.4	292	224	298	85	0	98	44	54.5

along a similar track. This flight was made in the upper troposphere region (altitudes 8 to 14 km) for most of the time and had a ~ 4 h of daytime and another ~ 4 h of nighttime measurements. The case studies shown here are taken from the daytime measurement. The strong event occurred at 57° N, 116° W, and 7.6 km, the weak event occurred at 50° N, 112° W, and 7.6 km, and the non-event was found in a similar geographical region, 52° N, 113° W, and 8.0 km (and thus all three events took place at similar temperatures < 240 K). Figure 3 shows the average aerosol size distributions taken for the periods corresponding to these three events (Fig. 2).

There are substantial differences in the number concentration and size distribution between all three of these events. The strong event had N_{4-9} of 1500 cm^{-3} and N_{4-2000} of 2000 cm^{-3} , the weak event had N_{4-9} of 20 cm^{-3} and N_{4-2000} of 60 cm^{-3} , and the non event had N_{4-9} of 5 cm^{-3} and N_{4-2000} of 100 cm^{-3} (failing to satisfy one of the NPF criteria, the ratio of N_{4-9} over N_{4-2000} ($N_{\text{Frac}} > 6\%$). The strong event shows clearly fresh new particles in the size range < 10 nm as does the weak event, but the strong event has a much higher particle concentrations for the smaller particles and the weak event has peaks at 20 nm and 70 nm. The non-event shows almost no particles in the < 10 nm range and shows more aged aerosols with the highest aerosol mode at around 70 nm. RHI was actually highest (20%) for the non-event compared to the weak event (15%) and strong event (8%) case. The surface area was comparable ($\sim 1 \mu\text{m}^2 \text{ cm}^{-3}$) for all three events. The surface areas measured at event times are often related to altitudes, with higher surface areas at lower altitudes (Young et al., 2007).

Differences among the three events can also be seen in the back trajectory data from HYSPLIT. The strong event had a higher amount of cumulative precipitation (12.4 mm) compared to the weak event (10.2 mm) and non event (1.8 mm) as is shown in Table 2. The solar flux was also slightly higher for the strong event (22.6 kW m^{-2}) than the weak-

(19.3 kW m^{-2}) and non-event (17.2 kW m^{-2}). However, the distinctive difference between the three events is the air mass history from the previous five days (Fig. 4). These trajectories show two main differences. The first difference is the altitude that the air masses come from. For the strong NPF event, the air mass originated from a much lower altitude (1 km) three days prior to the event, whereas the air mass for the weak event originated from about 2 km and the air mass for the non event was in the upper troposphere (7 km) for the past 5 preceding days. Furthermore, for the strong event, the air mass was uplifted over 6 km in the span of a day, whereas the air mass for the weak event rose 6 km in three days. Such differences suggest that the air mass from the strong NPF event underwent a significant extent of vertical motion and rapidly brought higher concentrations of the expected aerosol precursors (e.g., H_2SO_4 , NH_3 , organic compounds and water vapor, as well as OH and sulfur compounds that can be oxidized to form H_2SO_4 , including SO_2) from lower altitudes to aid in NPF at higher altitudes with lower temperatures. It is also possible that air mixing might occur when the humid and warm air was rapidly uplifted to higher altitudes and mixed with the cold and dry air at the higher altitudes and this case, a steep gradient of temperature and RH took place to enhance nucleation rates because nucleation is a non-linear process as discussed in Nilsson and Kulmala (1998). For the non-event, there was no uplifting present at all. It is noted that it was consistent that other non-event cases all did not have vertical motion, clearly underlying the importance of large scale vertical motion for nucleation in this high altitude region.

3.3 Case Study II (12 December 2005): Strong- and Weak-Events

Figures 5 and 6 show graphs for a strong and weak NPF event occurring on 12 December 2005. On 12 December 2005, the GV flew from Colorado (40° N latitude) south to latitude

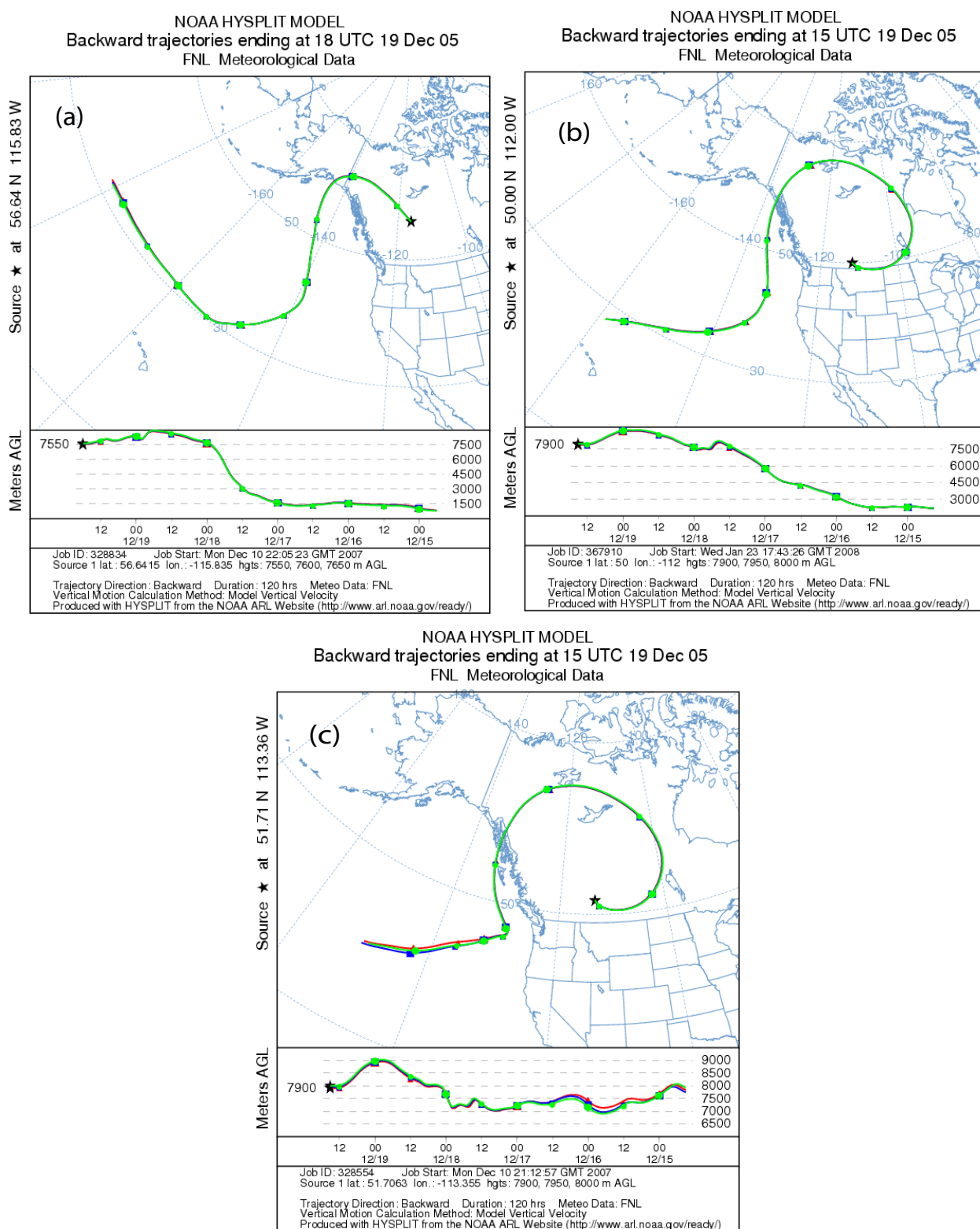


Fig. 4. NOAA HYSPLIT back trajectories for the airmasses for the strong- (upper left panels) (corresponding to Figs. 2a and 3a), weak- (upper right panels) (Figs. 2b and 3b), and non-event (bottom left panels) (Figs. 2c and 3c) on 19 December 2005. The star indicates where the event occurred. Altitude variations as a function of the number of days prior to the event are also shown (12 h of interval).

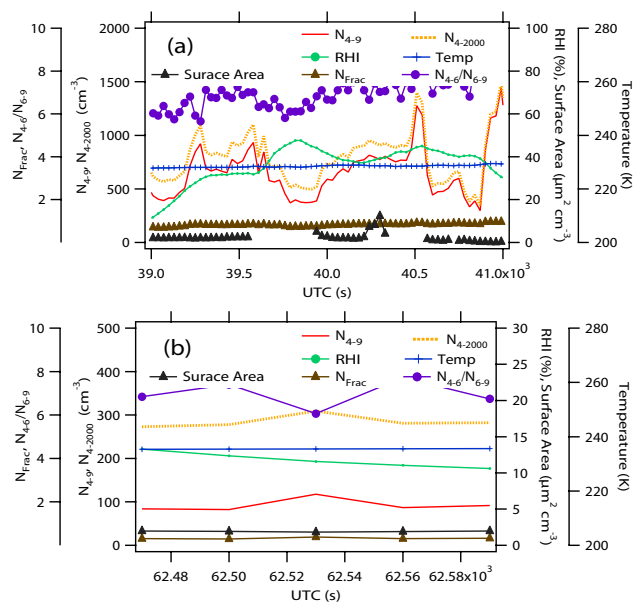


Fig. 5. The same as Fig. 2 except for a strong (a) and weak (b) NPF event occurring on 12 December 2005. The strong event occurred before sunrise (nighttime) at 36° N, 115° W, and 10 km. The weak event occurred during the day at 37° N, 111° W, and 9 km.

18° N before sunrise and returned along the same track to Colorado after sunrise by flying through similar longitudes, latitudes, and altitudes. The strong event occurred before sunrise (nighttime) at 36° N, 115° W, and 10 km while the weak event occurred after sunrise during the day at 37° N, 111° W, and 9 km. Both events occurred at temperatures below 240 K.

Similarly to the previous case study, there were substantial differences in number concentration and size distribution between the strong- and the weak-events. The strong event had N_{4-9} of 700 cm⁻³ and N_{4-2000} of 800 cm⁻³, whereas the weak event had N_{4-9} of 90 cm⁻³ and N_{4-2000} of 280 cm⁻³. The strong event also shows many more particles in the size range <10 nm, whereas the weak event shows similar amounts of smaller and larger particles. RHI was higher (40%) for the strong event compared to the weak event (12%). The surface area was also comparable ($\sim 2 \mu\text{m}^2 \text{cm}^{-3}$) for both events.

Once again the HYSPLIT trajectory shows differences between the two events. The strong event had a higher amount of cumulative precipitation (44 mm) compared to the weak event (8 mm) as is shown in Table 2. The solar flux, however, was comparable for both cases ($\sim 55 \text{ kW m}^{-2}$). The distinctive difference between the strong and weak events is the back trajectory from the previous five days (Fig. 7). These trajectories show the same differences as the previous case study. For the strong NPF event, the air mass originated from a much lower altitude (ground level) three days prior to

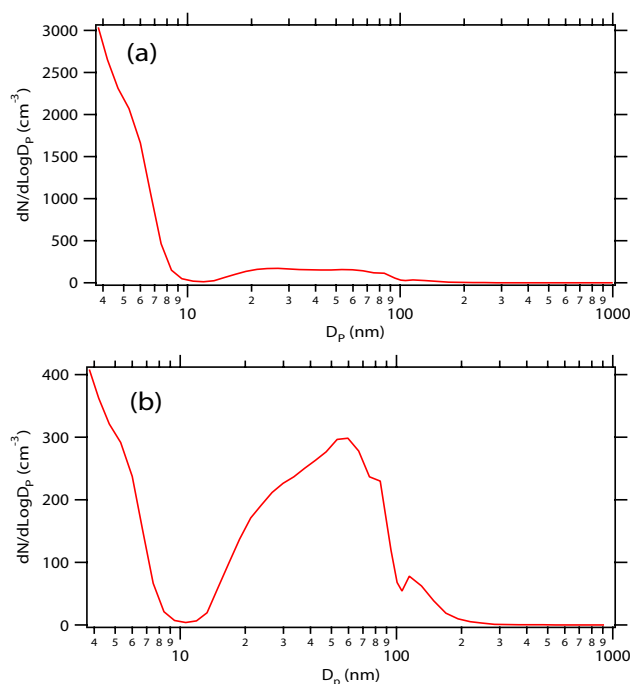


Fig. 6. The measured, average particle size distribution for the events from Fig. 5. The letters here correspond to those from Fig. 5 and each distribution is for the time period shown for the corresponding event from Fig. 5.

the event, whereas the air mass for the weak event was only exposed to altitudes as low as 7 km a day prior to the event and was actually at higher altitudes (~ 9 km) 2 to 3 days prior to the event. The strong event experienced rapid vertical motion (10 km in 2 days), whereas the weak event experienced far less an extent of vertical motion (only 2 km in a day). As in the previous case study, this could be a reason why the strong event had such high levels of new particle concentration compared to the weak event.

3.4 Latitude dependence of new particles

Figure 8 shows the latitude dependence of ultrafine particles for all 7 science flights measured at for three different temperature and altitude regions: temperature >250 K (altitude <6 km), 230 K < temperature < 250 K (6 km < altitude < 9 km), and 200 K < temperature < 230 K (9 km < altitude < 14 km). These results show that at altitudes from 9 to 14 km, particle concentrations are higher in the subtropics and mid-latitudes than in the tropics, consistent with the Hermann et al. (2003) trend; both the present study and Hermann et al. (2003) were mostly conducted near the tropopause region in the midlatitudes at similar latitude ranges. It has been shown that air mixing induced by convection and the stratosphere and troposphere exchange is strong in the mid-latitude (Pan et al., 2007) and these air mixing processes

the atmosphere is around 10–14 days under the typical free tropospheric conditions. Even with this relatively long photochemical lifetime, however, the measured SO_2 concentrations in the free troposphere showed a clear vertical profile, with much lower concentrations at higher altitudes than in the ground level (Thornton et al., 1999). In this case, uplifting can play a very important role for bringing higher concentrations of SO_2 from the source regions to higher altitudes in a short time. In addition, it is possible that rapid uplifting can also bring insoluble organic trace gases to higher altitudes to produce new particles (Kulmala et al., 2006). Abrupt air mixing can also take place during rapid uplifting. As shown in previous theoretical predictions (Nilsson and Kulmala, 1998), because nucleation is a non-linear process, when two air masses mix with each other with different RHI, temperatures, and aerosol precursors, nucleation rates can be much higher than without mixing.

While the role of uplifting of an air mass on NPF is much clear, it is less clear how other meteorological parameters from the air mass history can also play a role in determining if nucleation occurs and the extent to which it occurs (Table 2). The solar flux from the previous five days was similar for the strong- and weak- NPF events for both case studies and if the sun exposure fraction (that is the average ratio of the sun exposure hours in a day during the five preceding days) also did not vary much day to day (approximately 0.5 to 0.6), so the average OH concentrations in air masses would be similar. While the RHI was higher for the strong event than the weak event on 12 December, the values were comparable for both events on December 19 (Table 2). Precipitation may have affected the strength of the event as in both cases the strong event experienced more cumulative precipitation (Table 2). Precipitation is believed to lower the surface area density because of scavenging, but since for all these events the surface areas were in fact very low in this region, the precipitation effects can be less important under such a condition. For these specific case studies, however, the altitude rather seems to be a dominating factor in determining the strength of the NPF event. Both strong events had a median altitude of less than 2.5 km during the previous five days and had minimum altitudes very close to the ground level (<1 km), whereas for the weak events the median altitudes were both above 6 km and the air never fell below 2 km (Table 2). And, this may again point to the significance of air mass history in determining the extent of NPF.

It was consistent that weak- or non-events did not experience large scale uplifting during the Progressive Science Missions. Because of low surface areas and low temperatures, nucleation can easily take place, but with the limited supply of aerosol precursors in this region, nucleation becomes sensitive to the extent of vertical motion. Our observations are in line with numerous observations (de Reus et al., 1998; Nyeki et al., 1999; Ström et al., 1999; Twohy et al., 2002; Lee et al., 2003; Minikin et al., 2003; Hermann et al., 2003; Carslaw and Kärcher, 2006) in which NPF was of-

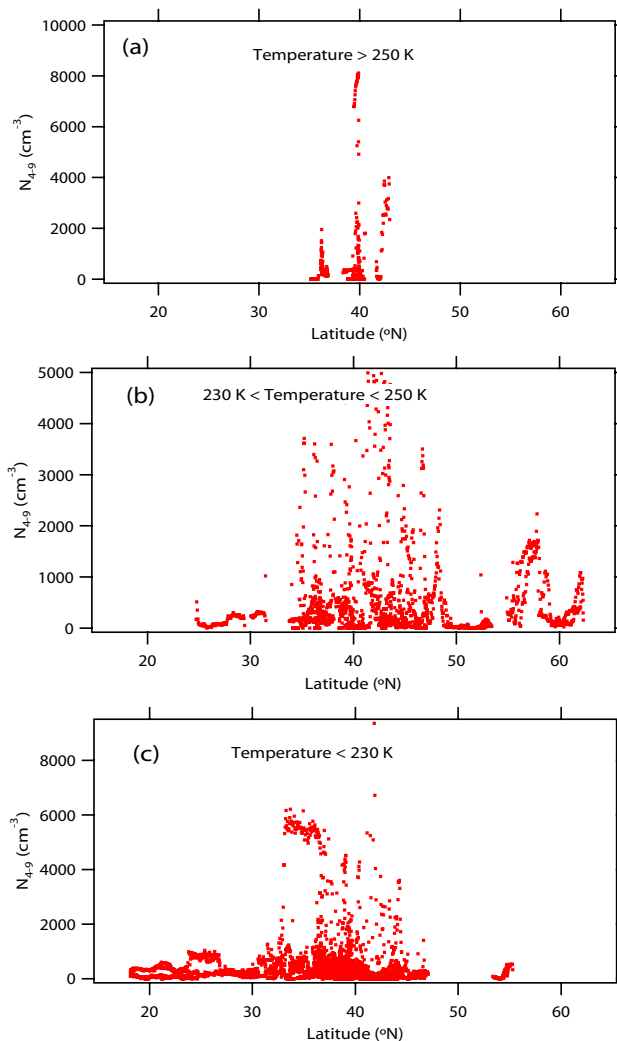


Fig. 8. The measured N_{4-9} as a function of latitude for different temperatures (and hence different altitudes) during the NSF/NCAR GV Progressive Science Mission. All 7 research flights are included here. Temperatures >250 K (Altitudes < 6 km); 230 K < Temperatures < 250 K (6 km < Altitudes < 9 km); Temperatures < 230 K (Altitudes > 9 km).

ten attributed to air mixing and convection. However, there were also some NPF cases where vertical motion clearly did not occur (<50% of the NPF cases), similarly to Young et al. (2007), suggesting that air mass history is an important but not the only governing factor for aerosol nucleation in this region.

Acknowledgements. This study was supported by NSF grants awarded to KSU (ATM-0507709; CAREER ATM-0645567). NCAR is supported by NSF, but any opinions expressed here do not represent those from NSF. We thank James C. Wilson for providing NMASS and FCAS and helpful discussions, and the scientists, engineers and pilots involved in the NSF/NCAR GV Progressive Science Missions. We also thank two reviewers for helpful comments.

Edited by: D. Cziczko

References

- Brock, C. A., Schröder, F., Kärcher, B., Petzold, A., Busen, R., and Fiebig, M.: Ultrafine particle size distributions measured in aircraft exhaust plumes, *J. Geophys. Res.*, 105, 26 555–26 567, 2000.
- Carslaw, K. S. and Kärcher, B.: Stratospheric aerosol processes, Chap. 1, in: *Stratospheric Processes and Their Role in Global Climate (SPARC), A Project of WMO/ICSU/IOC World Climate Research Program: Assessment of Stratospheric Aerosol Properties (ASAP)*, edited by: Thomason, and Peter, Th., SPARC Scientific Steering Group, February 2006, <http://www.atmosp.physics.utoronto.ca/SPARC/ASAP%20V3c1.pdf>, 2006.
- de Reus, M., Ström, J., Kulmala, M., Pirjola, L., Lelieveld, J., Schiller, C., and Zöger, M.: Airborne aerosol measurements in the tropopause region and the dependence of NPF on preexisting number concentration, *J. Geophys. Res.*, 103, 31 255–31 263, 1998.
- de Reus, M., Ström, J., Hoor, R., Lelieveld, J., and Schiller, C.: Particle production in the lowermost stratosphere by convective lifting of the tropopause, *J. Geophys. Res.*, 104, 23 935–23 940, 1999.
- Draxler, R. R. and Rolph, G. D.: HYSPLIT (HYbrid Single-Particle Lagrangian Integrated Trajectory) Model access via NOAA ARL READY Website (<http://www.arl.noaa.gov/ready/hysplit4.html>), NOAA Air Resources Laboratory, Silver Spring, MD, 2003.
- Hermann, M., Heintzenberg, J., Wiedensohler, A., Zahn, A., Heinrich, G., and Brenninkmeijer, C. A. M.: Meridional distributions of aerosol particle number concentrations in the upper troposphere and lower stratosphere obtained by Civil Aircraft for Regular Investigation of the Atmosphere Based on an Instrument Container (CARIBIC) flights, *J. Geophys. Res.*, 108, 4114, doi:10.1029/2001JD001077, 2003.
- Jonsson, H. H., Wilson, J. C., Brock, C. A., Knollenberg, R. G., Newton, R., Dye, J. E., Baumgardner, D., Borrmann, S., Ferry, G. V., Pueschel, R., Woods, D. C., and Pitts, M. C.: Performance of a focused cavity aerosol spectrometer for measurements in the stratosphere of particle size in the 0.06–2.0 μm diameter range, *J. Atmos. Ocean Technol.*, 12, 115–129, 1995.
- Kulmala, M., Reissell, A., Sipilä, M., Bonn, B., Ruuskanen, T. M., Lehtinen, K. E. J., Kerminen, V.-M., and Ström, J.: Deep convective clouds as aerosol production engines: Role of insoluble organics, *J. Geophys. Res.*, 111, D17202, doi:10.1029/2005JD006963, 2006.
- Lee, S. H., Reeves, J. M., Wilson, J. C., Hunton, D. E., Viggiano, A. A., Miller, T. M., Ballenthin, J. O., and Lait, L. R.: Particle formation by ion nucleation in the upper troposphere and lower stratosphere, *Science*, 301, 1886–1889, 2003.
- Lee, S.-H., Wilson, J. C., Baumgardner, D., Herman, R. L., Weinstock, E. M., LaFleur, B. G., Kok, G., Anderson, B., Lawson, P., Baker, B., Strawa, A., Pittman, J. V., Reeves, J. M., and Bui, T. P.: NPF observed in the tropical/subtropical cirrus clouds, *J. Geophys. Res.*, 109, D02009, doi:10.1029/2004JD005033, 2004.
- Lee, S.-H., Young, L.-H., Benson, D. R., Suni, T., Kulmala, M., Junninen, H., Campos, T. L., Rogers, D. C., and Jensen, J.: Observations of Nighttime NPF in the Troposphere, *J. Geophys. Res.*, 113, D10210, doi:10.1029/2007JD009351, 2008.
- Mertes, S., Galgon, D., Schwirn, K., Nowak, A., Lehmann, K., Massling, A., Wiedensohler, A., and Wiegprecht, W.: Evolution of particle concentration and size distribution observed upwind, inside and downwind hill cap clouds at connected flow conditions during FEBUKO, *Atmos. Environ.*, 39, 4233–4245, 2005.
- Minikin, A., Petzold, A., Ström, J., Krejci, R., Seifert, M., Velthoven, P. V., Schlager, H., and Schumann, U.: Aircraft observations of the upper tropospheric fine particle aerosol in the northern and southern hemispheres at midlatitudes, *Geophys. Res. Lett.*, 30, 1503, doi:10.1029/2002GL016458, 2003.
- Nilsson, E. D. and Kulmala, M.: The potential for atmospheric mixing processes to enhance binary nucleation rate, *J. Geophys. Res.*, 103, 1381–1389, 1998.
- Nyeki, S., Kalberer, M., Lugauer, M., Weingartner, E., Petzold, A., Schröder, F., Colbeck, I., and Baltensperger, U.: Condensation Nuclei (CN) and ultrafine CN in the free troposphere to 12 km: A case study over the Jungfraujoch high-alpine research station, *Geophys. Res. Lett.*, 26, 2195–2198, 1999.
- Pan, L. L., Bowman, K. P., Shapiro, M., Randel, W. J., Gao, R., Campos, T., Davis, C., Schauffler, S., Ridley, B. A., Wei, J. C., and Barnet, C.: Chemical behavior of the tropopause region observed during the Stratosphere-Troposphere Analyses of Regional Transport (START) experiment, *J. Geophys. Res.*, 112, D18110, doi:10.1029/2007JD008645, 2007.
- Ström, J., Fischer, H., Lelieveld, J., and Schröder, F.: In situ measurements of microphysical properties and trace gases in two cumulonimbus anvils over western Europe, *J. Geophys. Res.*, 104, 12 221–12 226, 1999.
- Thornton, D. C., Bandy, A. R., Blomquist, B. W., Driedger, A. R., and Wade, T. P.: Sulfur dioxide distribution over the Pacific Ocean 1991–1996, *J. Geophys. Res.*, 104, 5845–5854, 1999.
- Twohy, C. H., Clement, C. F., Gandrud, B. W., Weinheimer, A. J., Campos, T. L., Baumgardner, D., Brune, W. H., Faloon, I., Sachse, G. W., Vay, S. A., and Tan, D.: Deep convection as a source of new particles in the midlatitude upper troposphere, *J. Geophys. Res.*, 107, 4560, doi:10.1029/2001JD000323, 2002.
- Wiedensohler, A., Hansson, H.-C., Orsini, D., Wendisch, M., Wagner, F., Bower, K. N., Choulaton, T. W., Wells, M., Parkin, M., Acker, A., Wiegprecht, W., Fachini, M. C., Lind, J. A., Fuzzi, S., Arends, B. G., and Kulmala, M.: Nighttime formation and occurrence of new particles associated with orographic clouds, *Atmos. Environ.*, 31, 2545–2559, 1997.
- Young, L.-H., Benson, D. R., Montanaro, W. M., Lee, S.-H., Pan, L. L., Rogers, D. C., Jensen, J., Stith, J. L., Davis, C. A., Campos, T. L., Bowman, K. P., Cooper, W. A., and Lait, L. R.: Enhanced NPF observed in the northern midlatitude tropopause region, *J. Geophys. Res.*, 112, D10218, doi:10.1029/2006JD00810, 2007.